JOURNAL OF APPLIED ELECTROCHEMISTRY **28** (1998) 41–48

Intercalation of lithium in r.f.-sputtered vanadium oxide film as an electrode material for lithium-ion batteries

N. KUMAGAI, H. KITAMOTO, M. BABA

Faculty of Engineering, Iwate University, Ueda 4-3-5, Morioka 020 Japan

S. DURAND-VIDAL, D. DEVILLIERS, H. GROULT

Universite Pierre et Marie Curie, Laboratoire LI2C-Electrochimie, 4 place Jussieu, 75252 Paris, France

Received 13 January 1997; revised 21 July 1997

Vanadium oxide films were prepared by r.f.-sputtering using an argon sputter gas and a V_2O_5 target. The films were characterized by scanning electron microscopy, atomic force microscopy, X-ray diffraction, X-ray photoelectron spectroscopy and electrochemical techniques. The oxide film as deposited is amorphous; they are heat-treated in the range 300–700 °C in oxygen atmosphere and are composed of orthorhombic V_2O_5 crystals. At higher heat-treatment temperatures (600–700 °C) the crystallization of the oxide proceeded significantly with *ab*-direction parallel to the substrate. The oxide film undergoes a reversible lithium intercalation and deintercalation process. The kinetics of the intercalation process of lithium into amorphous V_2O_5 film was studied using an a.c. impedance method. Furthermore, a rocking-chair type V_2O_5 film/$Li_xV_2O_5$ film cell could be charge–discharge cycled over 300 times at a current of 10 μA at 25 °C.

Keywords: *lithium intercalation*, *vanadium oxide thin film*, *lithium-ion batteries*

1. Introduction

Considerable attention has recently been devoted to the investigation of the lithium metal-free rocking chair batteries, such as $Li_xC/Li_{1-x}CoO_2$ couples. We have previously reported the electrochemical, structural and kinetic characteristics of V_2O_5 electrodes with lithium intercalation into the crystal lattice [1–3]. West *et al*. have studied lithium insertion in sputtered vanadium oxide films [4]. Furthermore, we have reported the electrochemical characteristics of Nb_2O_5 thin films, prepared by r.f-sputtering, as an electrode material for lithium-ion batteries [5].

In the present work, V_2O_5 thin films prepared by r.f. sputtering have been characterized by several methods and the electrochemical lithium intercalation in V_2O_5 thin film has been examined by galvanostatic and a.c. impedance methods. Furthermore, metallic lithium-free rocking chair batteries, consisting of $Li_xV_2O_5$ films and V_2O_5 films as the negative and positive electrodes, respectively, have been constructed and the charge–discharge cycling behaviour has been examined.

2. Experimental details

Thin films of vanadium oxide were deposited on SUS 304 stainless steel substrates (thickness 0.05 mm) and P-type Si(1 0 0) substrates using an r.f. (13.56 MHz) sputtering method in an argon atmosphere (Anelva, SPF-210B). The r.f. power was in the range 200 to 50 W and the argon pressure was in the range 60 to 100 m torr. A pressed and sintered 99.9% V_2O_5 target was used as the source of evaporation. The oxide films were heat-treated in the temperature range 200 to 700 °C in oxygen atmosphere for 1 h. The surface area of the vanadium oxide layer was 1.0 cm^2. The thickness of the vanadium oxide film was measured by observing interference fringes, using a multiple-beam interferometer (Mizojiri, type II). The weight of the vanadium oxide layer was calculated using the density of V_2O_5 (3.36 g cm^{-3}). The characterization of the oxide films was carried out by means of scanning electron microscopy (SEM) (Hitachi S-450), atomic force microscopy (AFM) (Digital Instruments, Nanoscope III, tapping mode) and X-ray diffractometry (XRD) (Rigaku Denki Geiger flex 20B, CuK_α and X-ray photoelectron (ESCA) spectroscopy (Ulvac-phi ESCA 5600CI). To investigate the electrochemical properties, an electrochemical cell was constructed by coupling the oxide film with a lithium counter electrode and a lithium reference electrode in a 1 M $LiClO_4$–propylene carbonate (PC) electrolyte, containing a small amount of water (less than 20 mg dm^{-3}). A glass beaker-type cell was used as an electrochemical cell. All the measurements were carried out in a dry box filled with argon. A.c. impedance measurements were performed using NF Electronic Instrument 5720B frequency response analyser, Tohogiken potentiostat 2000 and HP 9000-200 microcomputer. A 5 mV r.m.s. perturbation was supplied in the frequency range 10^5–10^{-3} Hz.

0021-891X

3. Results and discussion

3.1. *Structure of the vanadium oxide film prepared by r.f.-sputtering*

The SEM photographs of the vanadium oxide films on the silicon substrate heat-treated at various temperatures in oxygen atmosphere are shown in Fig. 1. The oxide films were prepared by r.f.-sputtering at 100W and 80 m torr. As can be seen, the vanadium oxide crystals grow in the temperature range from 600 to 700 °C and the surface of the oxide film is fairly flat at a higher temperature of 700 °C.

Typical AFM images for the vanadium oxide films deposited on the stainless steel substrate by r.f.-sputtering at 100 W and 80 m torr, and then heat treated at 500 °C and 700 °C for 1 h in oxygen, are given in Fig. 2. At temperatures below 500 °C the oxide film was aggregated of small spherical particles with a diameter of about 0.1 μm (Fig. 2(a)). By contrast, at a higher temperature of 700 °C, the crystallization of the oxide film proceeded significantly, as seen in Fig. 2(b).

The crystals with a layered structure grew preferentially with *ab*-plane parallel to the substrate. The X-ray diffraction patterns of the vanadium oxide films heat-treated at various temperatures are given in Fig. 3. The oxide films were prepared on the Si substrate by r.f.-sputtering at 100 W and 80 m torr. The oxide films, as deposited, were amorphous without any significant V_2O_5 peak. The crystalline V_2O_5 phase appeared with heat-treatment above 200 °C. These X-ray patterns are identical with V_2O_5 having an orthorhombic structure (Pmmn, $a = 1151$ pm $b = 355.9$ pm, $c = 437.1$ pm, $Z = 2$ [6]) as shown in Fig. 4. However, the patterns showed large deviation in relative peak intensity from the standard pattern of polycrystalline V_2O_5 powder having an orthorhombic system [1]. The intensity of the (1 1 0) diffraction peak tends to increase with increase in heat-treatment temperature from 200 to 500 °C. This indicates that, as the heat-treatment temperature increases, the crystallites of the oxide film grow preferentially with the *ab*-plane perpendicular to the silicon substrate. However, at a higher temperature above 600 °C, the intensity of the (0 0 1) peak increased considerably, showing

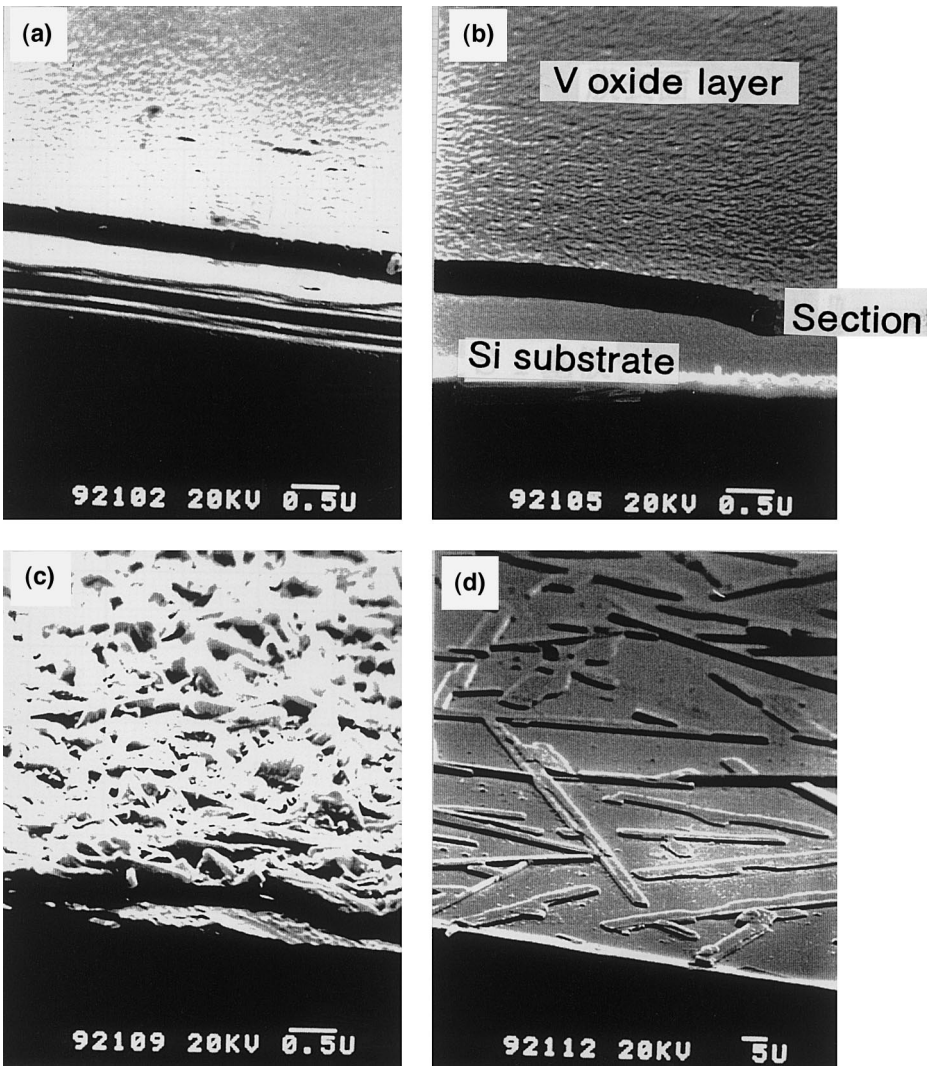

Fig. 1. Scanning electron micrographs of vanadium oxide films on silicon substrate heat-treated at various temperatures for 1 h in oxygen. (a) as deposited, (b) 500 °C, (c) 600 °C and (d) 700 °C.

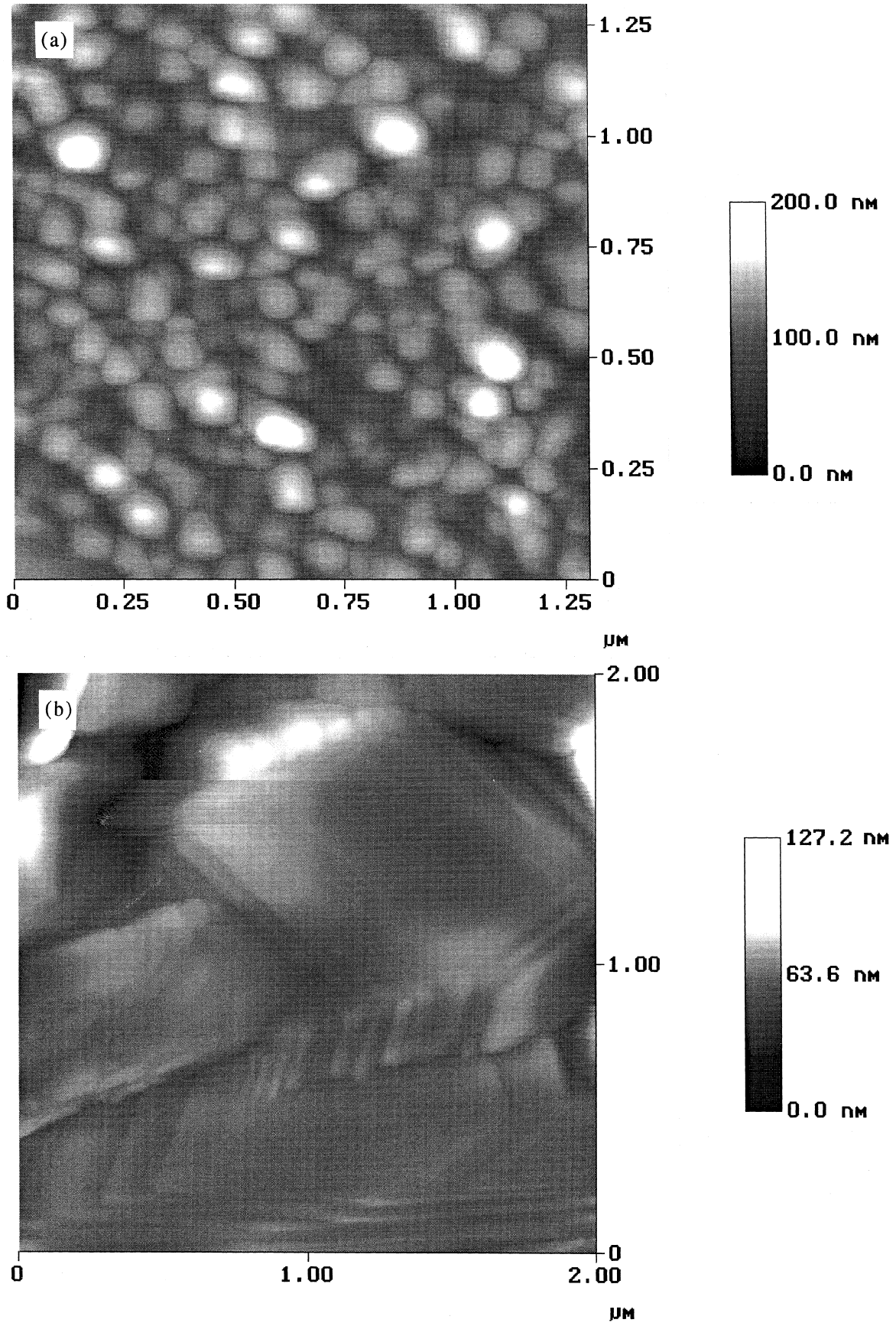

Fig. 2. Atomic force microscopy images for vanadium oxide films on the stainless steel-substrate heat treated at several temperatures for 1 h in oxygen. (a) 500 °C and (b) 700 °C.

that the crystallites grow with the *ab* plane parallel to the substrate. The XRD patterns of the vanadium oxide films, deposited at different sputtering conditions and then heat-treated at 500 °C for 1 h in oxygen atmosphere, are given in Fig. 5. The crystallization of the oxide proceeded with an increase in r.f. power.

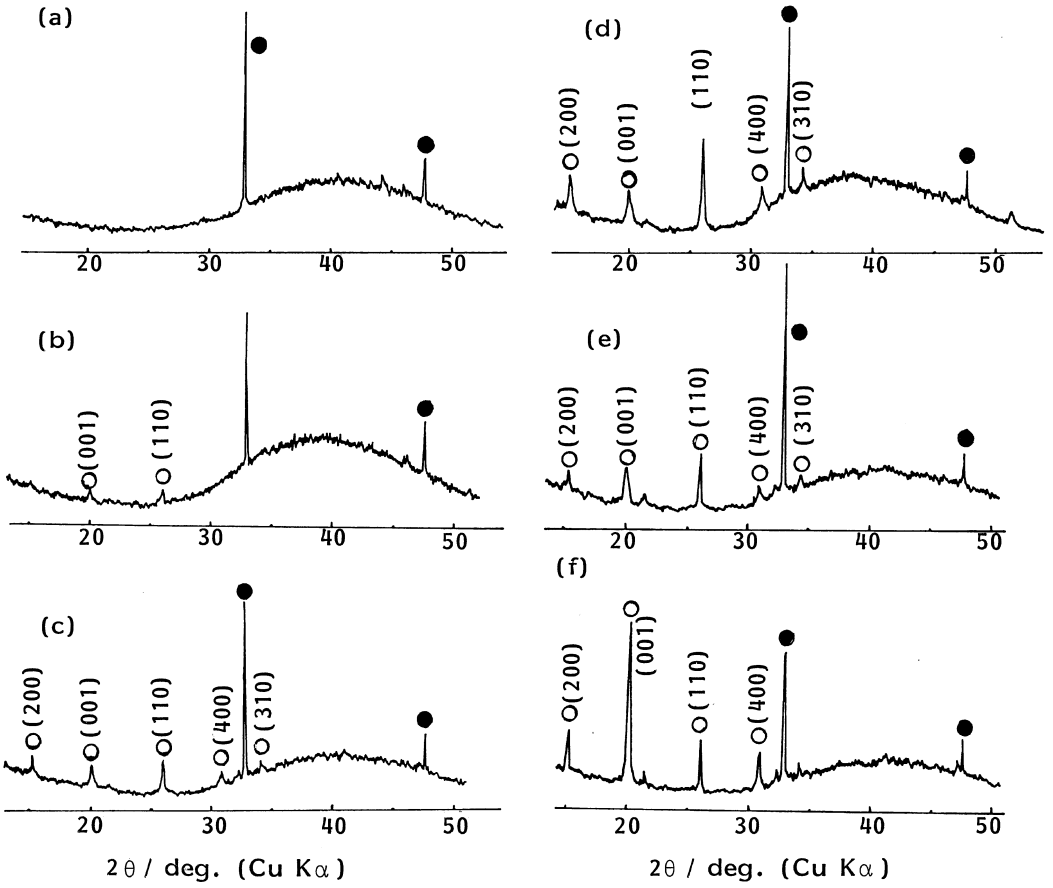

Fig. 3. X-ray diffraction patterns of vanadium oxide films heat-treated at various temperatures for 1 h in oxygen. (a) as deposited, (b) 200 °C, (c) 300 °C, (d) 400 °C (e) 500 °C and (f) 600 °C. Key: (O) V_2O_5 and (●) Si.

The surface chemical composition of the vanadium oxide film as deposited on the stainless-steel at 100 W and 80 m torr in argon was first examined by ESCA spectroscopy. The thickness of the oxide film used was 370 nm. The composition obtained was $V_2O_{4.84}$. This reveals deviation from the ideal stoichiometry and the presence of high concentration of oxygen defects. Furthermore, the vanadium oxide film was electrochemically intercalated up to $x = 2$ in $Li_xV_2O_5$ at 0.01 mA cm^{-2} in 1 M $LiClO_4$–PC. The lithiated oxide film, after washing with PC and drying in vacuum, was analysed by ESCA spectroscopy. The composition of the oxide film is shown as a function of argon sputter time (i.e. thickness) in Fig. 6. At the surface of the film chlorine and carbon atoms were detected, due to the decomposition products of the electrolyte, but in the inner layer only O, V and Li atoms were detected during argon sputtering for 220 min, corresponding to the thickness of 370 nm. The composition of the oxide film at the thickness of 5 nm was $Li_{2.06}V_2O_{4.83}$, in which the lithium content approximately agrees with that calculated from the quantity of electricity to prepare the compound.

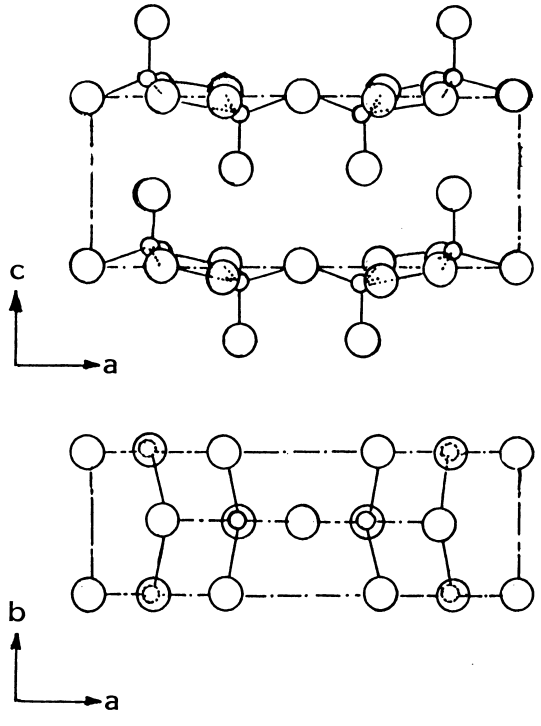

Fig. 4. Crystal structure of V_2O_5. Key: (small circle) V atom; (large circle) O atom.

3.2. *Electrochemical behaviour of r.f.-sputtered vanadium oxide film*

Figure 7 shows the discharge curves of vanadium oxide films heat-treated at various temperatures for 1 h in oxygen. The oxide films were obtained by r.f.-sputtering at 100 W and 80 m torr for 4 h on the stainless steel substrate, and the discharge curves

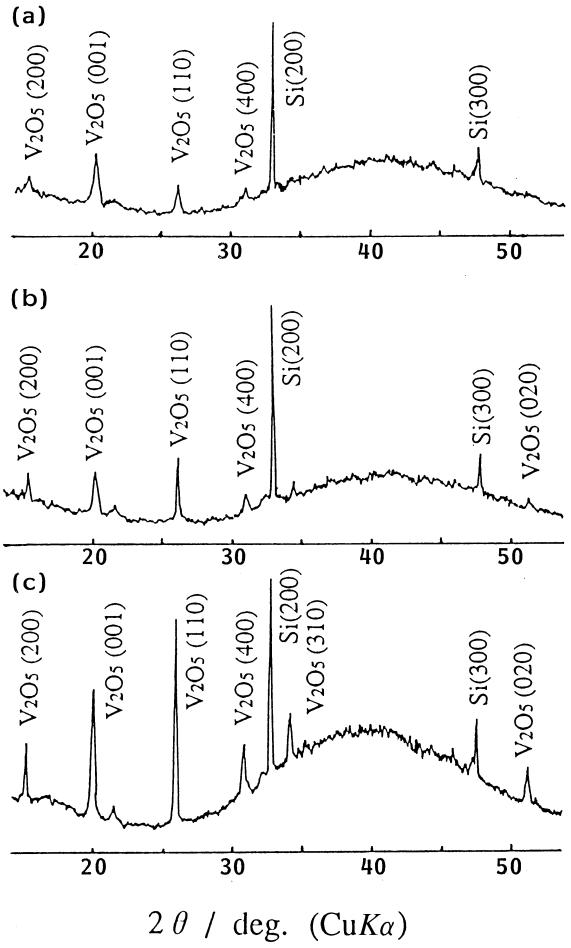

Fig. 5. X-ray diffraction patterns of vanadium oxide films prepared on Si substrate at different sputtering conditions and heat-treated at 500 °C for 1 h in oxygen. Sputtering conditions: (a) 50 W, 100 mtorr (Ar), 7 h; (b) 100 W, 80 mtorr (Ar), 4 h; (c) 200 W 60 m torr (Ar), 1.5 h.

were measured at a current density of 10 μA cm^{-2} in 1 M $LiClO_4$–PC at 25 °C. The amorphous oxide film, as deposited, showed a monotonic decrease in potential with lithium incorporation, giving an initial discharge capacity of about 400 mAh (g oxide)$^{-1}$ corresponding to 3 Li mol^{-1} of the oxide. On the other hand, the oxide film heat-treated at 300 ~ 400 °C for 1 h in oxygen atmosphere showed stepwise discharge curves including a high potential plateau around 3.3 V and gave a discharge capacity of about 370 mAh (g oxide)$^{-1}$. This electrochemical behaviour is similar to that of the crystalline V_2O_5 powder pressed electrode given in Fig. 8 for comparison; however a large decrease in the discharge capacity above 3 V is observed. This shows that the oxide film heat-treated at 300 ~ 400 °C contains an appreciable amount of reduced vanadium ion such as V^{4+}. When the heat-treatment temperature of the oxide film was raised to 500 ~ 600 °C, the high potential plateau around 3.3 V almost disappeared, resulting in a single S-shape curve. However, the capacity decreased considerably at a higher temperature of 600 °C, where highly crystallized V_2O_5 strongly orientated with the *ab* plane parallel to the substrate is formed. The discharge curves of vanadium oxide films prepared at different sputtering conditions are also shown in Fig. 8, as well as the curve obtained with crystalline V_2O_5 powder pressed electrode given for comparison. These oxide films were heat-treated at 500 °C for 1 h in oxygen. The oxide film obtained at a low r.f. power of 50 W showed a stepwise discharge behaviour similar to the crystalline V_2O_5 electrode, while the one prepared at a higher r.f. power of 100 ~ 200 W gave a single S-shape curve, similar to the discharge behaviour of the oxide film heat

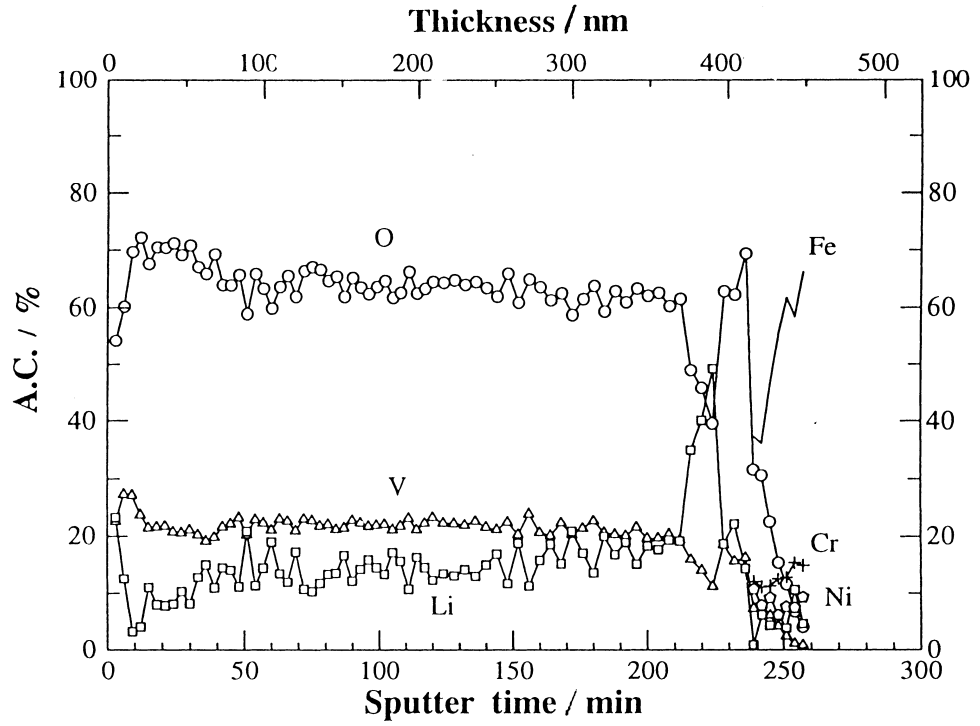

Fig. 6. The composition of vanadium oxide films on the stainless-steel substrate as a function of sputter time.

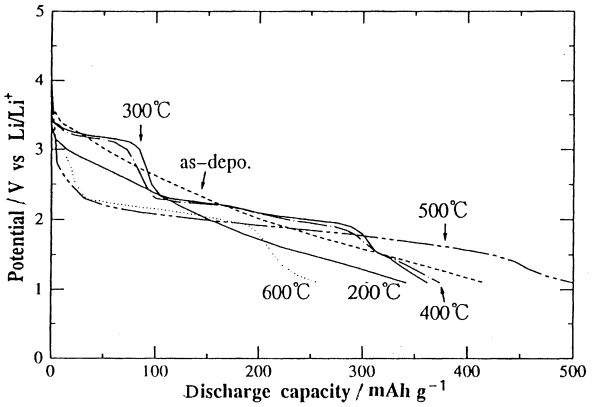

Fig. 7. Initial discharge curves of vanadium oxide films heat-treated at various temperatures for 1 h in oxygen. Current density 10 μA cm^{-2}.

treated at 500 ~ 600 °C (Fig. 7). Thus, the discharge behaviour of the vanadium oxide films strongly depends on sputtering conditions and heat-treatment temperature.

The charge–discharge cyclic curves of several vanadium oxide films as deposited and heat-treated at 300 °C are shown in Figs 9 and 10. The V_2O_5 films were obtained by r.f.-sputtering at 100 W and 80 m torr. The discharge capacity of the amorphous oxide film as deposited (a) decreased gradually on cycling up to 30 times in the potential range from 1.1 to 4.4 V, while on cycling in the wider potential range from 0.1 to 4.0 V (b), the oxide film showed considerably higher discharge capacity of about 800 mAh (g oxide)$^{-1}$ during 30 cyclings. In the vanadium oxide films heat-treated at a temperature of 300 ~ 400 °C (Fig. 10), the major change in the discharge behaviour occurred after the first cycling, resulting in monotonic decrease in the discharge potential on further cycling, which is similar to the discharge behaviour of the amorphous V_2O_5 film. The major change in the discharge behaviour caused by the initial discharge and recharge may be due to the irreversible structural variation to a more disordered phase [1]. In spite of the major structural change in

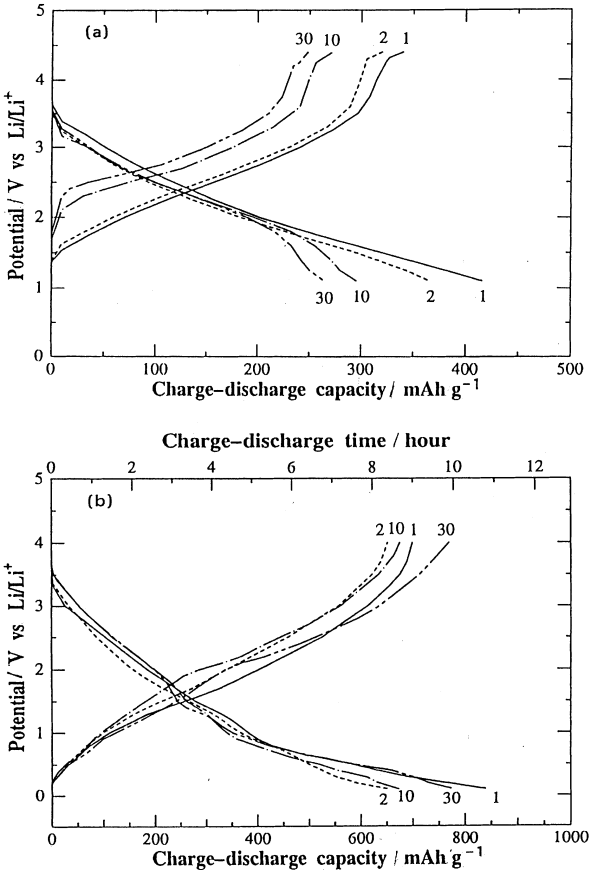

Fig. 9. Charge–discharge cyclic curves of vanadium oxide films as deposited. Current density 0.01 mA cm^{-2}. The oxide electrodes were cycled between the potentials of 1.1 and 4.4 V in (a) and between the potentials of 0.1 and 4.0 V in (b).

the initial cycling, a high capacity of about 300 mAh (g oxide)$^{-1}$ was obtained during 30 cyclings.

Sputtered V_2O_5 films with a thickness of 380 nm and a surface of 1 cm^2 as deposited on stainless steel substrate in argon were used as both the positive and negative electrodes for the rocking-chair V_2O_5/$Li_xV_2O_5$ cell. For the preparation of the negative electrode, the V_2O_5 film was at first electrochemically lithiated up to a potential of 0.1 V vs Li/Li$^+$ in 1 M $LiClO_4$–PC. Fig. 11(a) shows the charge–discharge

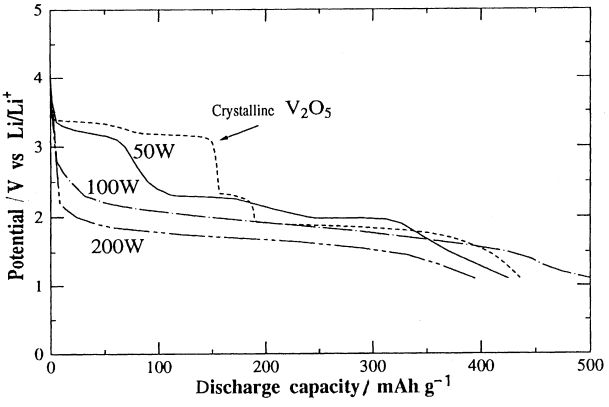

Fig. 8. Initial discharges curves of vanadium oxide films prepared at different sputtering conditions. Current density 10 μA cm^{-2}. Sputtering conditions: (a) 50 W, 100 mtorr (Ar), 7 h; (b) 100 W, 80 mtorr (Ar), 4 h; (c) 200 W 60 mtorr (Ar), 1.5 h.

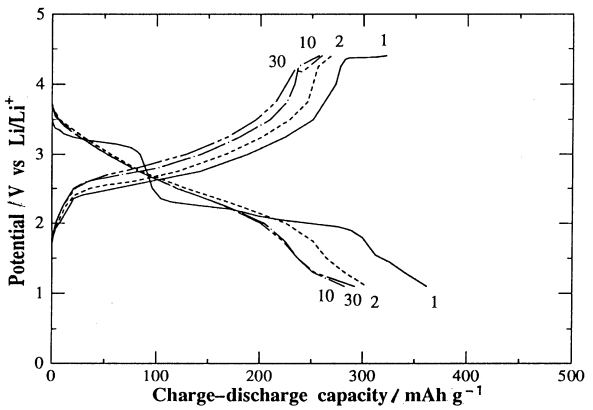

Fig. 10. Charge–discharge cyclic curves of vanadium oxide films heat-treated at 300 °C for 1 h in oxygen. Current density 10 μA cm^{-2}.

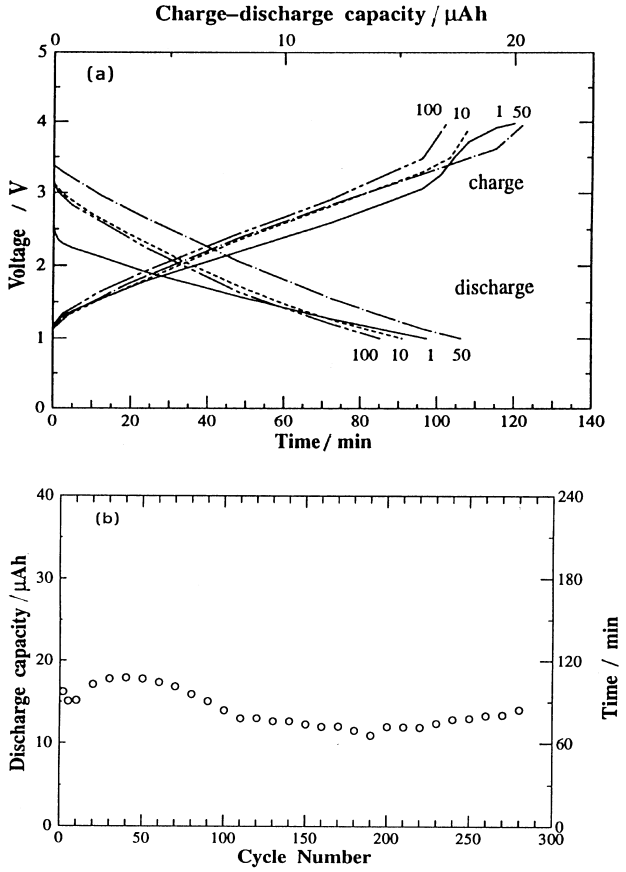

Fig. 11. Cycling performance of V_2O_5 film /$Li_xV_2O_5$ film cell. V_2O_5 film (380 nm, 1.0 cm^2) as-deposited. Current 10 $\mu A\,cm^{-2}$. Sputtering conditions 100 W, 80 mtorr (Ar).

cyclic curves of the V_2O_5 film/$Li_xV_2O_5$ film cell containing 1 M $LiClO_4$–PC, measured at a current of 10 μA and 25 °C. The variation in the discharge capacity of the cell is given in Fig. 11(b) as a function of cycle number. Over 300 charge-discharge cycles were possible at a voltage of $3.0 \sim 1.0$ V with a capacity of about 15 μAh. This capacity was about twice larger than that for the V_2O_5 film/$Li_2Nb_2O_5$ film cell [5]. The V_2O_5 positive electrode was cycled in a high potential range from 2.5 to 4 V vs Li/Li^+ during charge–discharge cycling, while the $Li_xV_2O_5$ negative electrode was cycled in a considerably lower potential range from 0.1 to 1.5 V vs Li/Li^+. Furthermore, when the $V_2O_5/Li_xV_2O_5$ rocking-chair cell having thicker V_2O_5 films of 650 nm was devoted to charge–discharge cycling, a similar cell performance with a capacity of about 15 μAh was obtained during 200 cyclings. The low utilization of the thicker oxide film is mainly due to slow lithium diffusion in the oxide matrices.

The a.c. impedance spectra of $Li_xV_2O_5$ films were measured at various x-values in 1 M $LiClO_4$–PC at 40 °C. The oxide film was prepared by r.f. sputtering at 100 W and 80 m torr. Fig. 12(a) shows a typical impedance spectrum for $Li_{0.5}V_2O_5$ film. The response mainly consists of two low frequency spikes having angles of about 45° and about 90° against the real axis. This reveals that the discharge process is controlled by the lithium diffusion in the oxide matrices. The chemical diffusion coefficient of lithium, $\widetilde{D}$, in the oxide was obtained using the low frequency spike of about 45° from the following equations [7]:

$$Z_w = A_w \omega^{-1/2} \tag{1}$$

$$A_w = \frac{V_m(dE/dx)}{zFa\widetilde{D}^{1/2}} \tag{2}$$

where Z_w is the Warburg impedance, ω is the angular frequency of the a.c. perturbation, V_m is the molar volume of V_2O_5 (54.1 $cm^3\,mol^{-1}$), dE/dx is the slope of the open circuit potential against x-value in $Li_xV_2O_5$ curve and a is the electroactive surface area of the oxide electrode (1.0 cm^2). The Warburg prefactor, A_w, was obtained from the plot of the observed Warburg impedance $|Z_w|$ against $\omega^{-1/2}$ (Equation 1), as shown in Fig. 12(b). The chemical diffusion coefficient is related to the component diffusion coefficient for lithium, D_{Li}, by the following equation [8]:

$$\widetilde{D} = D_{Li}\frac{d\ln a_{Li}}{d\ln C_{Li}} = -D_{Li}\frac{F}{RT}\left(\frac{dE}{dx}\right) \tag{3}$$

where $(d\ln a_{Li}/d\ln C_{Li})$ is the thermodynamic enhancement factor, and R is the gas constant.

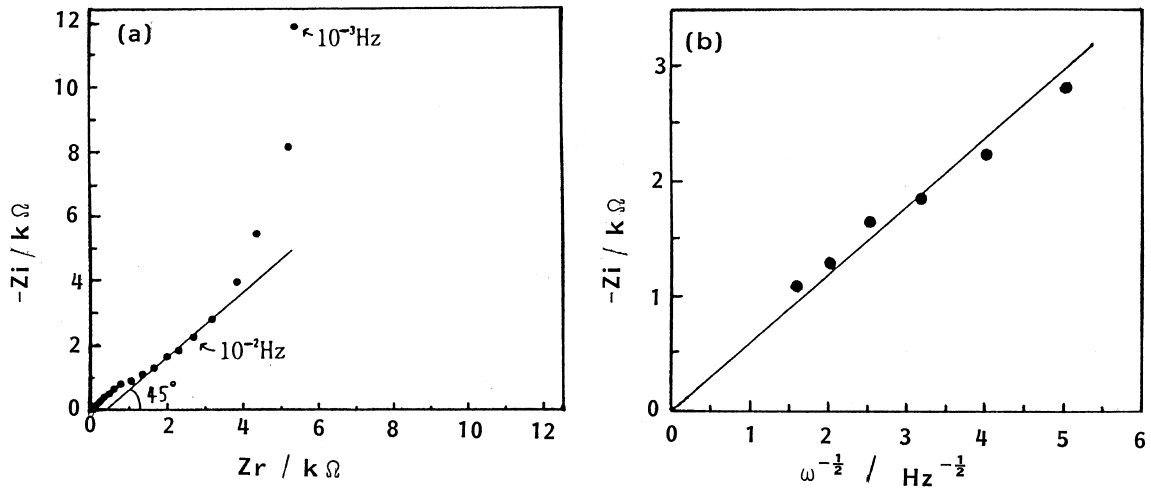

Fig. 12. Typical impedance diagram for $Li_{0.5}V_2O_5$ film (thickness 300 nm) (a) and plot of Warburg impedance $|Z_w|$ against $\omega^{-1/2}$ (b).

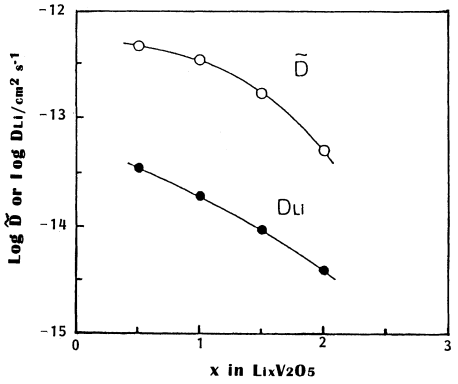

Fig. 13. Chemical ($\widetilde{D}$) and component (D_{Li}) diffusion coefficients of lithium in $Li_xV_2O_5$ at 40 °C.

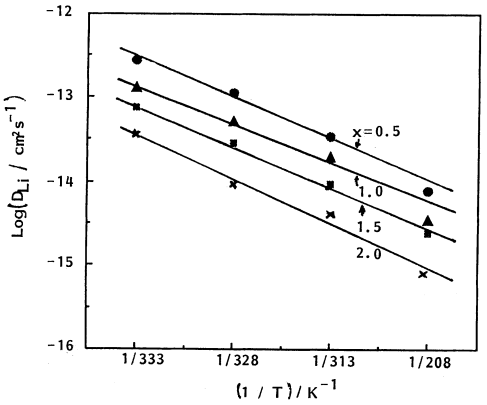

Fig. 14. Arrhenius plots of D_{Li} against T^{-1} for various x-values in $Li_xV_2O_5$.

The chemical diffusion coefficient $\widetilde{D}$ and lithium component diffusion coefficient D_{Li} at 40 °C are shown in Fig. 13, as a function of the x-value in $Li_xV_2O_5$. The $\widetilde{D}$ values are found to be of the order of $10^{-13} \sim 10^{-14}\,cm^2\,s^{-1}$ at 40 °C: these decrease with increasing x-value. These $\widetilde{D}$ values are higher than those of $Li_xNb_2O_5$ thin film (order of $10^{-14} \sim 10^{-15}\,cm^2\,s^{-1}$ at 25 °C and $x = 0 \sim 2$) [5] and Li_xMnO thin film ($2.2 \times 10^{-15}\,cm^2\,s^{-1}$ at 15 °C and $x = 0.02 \sim 0.06$) [9]. However, they are considerably lower than that of amorphous WO_3 thin film ($2.8 \times 10^{-11} \sim 2.4 \times 10^{-12}\,cm^2\,s^{-1}$ at 23 °C and $x = 0.1 \sim 0.26$) [7]. The lithium component diffusion coefficients, D_{Li}, were found to be of order $10^{-14} \sim 10^{-15}\,cm^2\,s^{-1}$ at 40 °C and to decrease proportionally with increase in the x-value. The D_{Li} value is related to the rate of random motion in the absence of a concentration gradient, so that the component diffusion coefficients are one order of magnitude lower than the $\widetilde{D}$ values. Furthermore, from the Arrhenius plots of the component diffusion coefficients for $Li_xV_2O_5$ ($x = 0.5 \sim 2$) films (Fig. 14), an activation enthalpy of $80 \sim 100\,kJ\,mol^{-1}$ was obtained.

Acknowledgements

The authors thank H. Shinada, Mrs Nobuko Kumagai and K. Ohta for their helpful assistance with the experimental work and Dr H. Yashiro for ESCA measurements.

References

[1] N. Kumagai and K. Tanno, *Denki Kagaku*, **48** (1980) 432.
[2] N Kumagai, K. Tanno, T. Nakajima and N. Watanabe, *Electrochim. Acta* **28** (1983) 17.
[3] N. Kumagai, I. Ishiyama and K. Tanno, *J. Power Sources* **20** (1987) 193.
[4] K. West, B. Zachau-Christiansen, S. V. Skaarup and F. W. Poulsen, *Solid State Ionics* **57** (1992) 41.
[5] N. Kumagai, Y. Tateshita, Y. Takatsuka, M. Baba, T. Ikeda and K. Tanno, *J. Power Sources* **54** (1995) 175.
[6] Joint Committee on Powder Diffraction Standards, 9-387.
[7] C. Ho, I. D. Raistrick and R. A. Huggins, *J. Electrochem. Soc.* **127** (1980) 343.
[8] W. Weppner and R. A. Huggins, *Ann. Rev. Mater. Sci.* **8** (1978) 269.
[9] L. Chen and J. Shoonman, *Solid State Ionics* **60** (1993) 227.